THE JOURNAL OF BIOLOGICAL CHEMISTRY
Vol. 277, No. 42, Issue of October 18, pp. 39477–39484, 2002

Printed in U.S.A.

The Role of Apolipoprotein A-I Helix 10 in Apolipoprotein-mediated Cholesterol Efflux via the ATP-binding Cassette Transporter ABCA1*

Received for publication, July 12, 2002, and in revised form, August 12, 2002
Published, JBC Papers in Press, August 13, 2002, DOI 10.1074/jbc.M207005200

Stacey E. Panagotopulos, Scott R. Witting, Erica M. Horace, David Y. Hui, J. Nicholas Maiorano, and W. Sean Davidson‡

From the Department of Pathology and Laboratory Medicine, University of Cincinnati, Cincinnati, Ohio 45267-0529

Recent studies of Tangier disease have shown that the ATP-binding cassette transporter A1 (ABCA1)/apolipoprotein A-I (apoA-I) interaction is critical for high density lipoprotein particle formation, apoA-I integrity, and proper reverse cholesterol transport. However, the specifics of this interaction are unknown. It has been suggested that amphipathic helices of apoA-I bind to a lipid domain created by the ABCA1 transporter. Alternatively, apoA-I may bind directly to ABCA1 itself. To better understand this interaction, we created several truncation mutants of apoA-I and then followed up with more specific point mutants and helix translocation mutants to identify and characterize the locations of apoA-I required for ABCA1-mediated cholesterol efflux. We found that deletion of residues 221–243 (helix 10) abolished ABCA1-mediated cholesterol efflux from cultured RAW mouse macrophages treated with 8-bromo-cAMP. Point mutations in helix 10 that affected the helical charge distribution reduced ABCA1-mediated cholesterol efflux *versus* the wild type. We noted a strong positive correlation between cholesterol efflux and the lipid binding characteristics of apoA-I when mutations were made in helix 10. However, there was no such correlation for helix translocations in other areas of the protein as long as helix 10 remained intact at the C terminus. From these observations, we propose an alternative model for apolipoprotein-mediated efflux.

Numerous studies have shown that high levels of high density lipoprotein (HDL)[1] and its most abundant protein constituent apolipoprotein A-I (apoA-I) can reduce the risk of atherosclerosis, the leading cause of death in industrialized countries (1). ApoA-I, a 28-kDa protein, is critical to HDL function in reverse cholesterol transport, the delivery of peripheral tissue cholesterol to the liver for catabolism. ApoA-I is thought to mobilize cellular cholesterol by at least two general mechanisms. The first is passive diffusion of cell membrane cholesterol down a concentration gradient to a phospholipid-containing lipoprotein (for a review, see Ref. 2). More recently, it has been shown that lipid-poor forms of apoA-I can actively remove cholesterol by directly interacting with the cell membrane to form a nascent HDL particle in a process called apolipoprotein-mediated lipid efflux (3–6).

Studies on a rare genetic disorder, Tangier disease, have shown that active apolipoprotein-mediated lipid transfer is necessary for the initial formation of the HDL particle. Tangier patients exhibit extremely low HDL levels and low plasma apoA-I and accumulate cholesteryl esters in many macrophage-containing tissues such as tonsils, lymph nodes, liver, and spleen (7). Genetic analyses on Tangier kindreds have implicated the ATP-binding cassette transporter-1 (ABCA1) as the molecular defect (8–10). It is likely that lipid-free apoA-I is rapidly cleared from plasma unless it becomes associated with lipid through interaction with the ABCA1 transporter, making the ABCA1/apoA-I interaction critical for the initial formation of HDL particles (11). Ensuing *in vitro* studies also suggested a primary role for ABCA1 in apolipoprotein-mediated cholesterol efflux in the periphery (12). For instance, cholesterol loading of macrophages and fibroblasts was shown to elevate mRNA of ABCA1, ABCA1 surface expression, apolipoprotein surface binding, and cholesterol efflux (13–16). Overexpression of ABCA1 using recombinant techniques increased apoA-I binding and cholesterol efflux (15, 17). In addition, cAMP was found to induce ABCA1 mRNA and protein in macrophages, which subsequently increased apoA-I binding and cholesterol efflux (16, 18).

However, the molecular basis for the interaction between ABCA1 and apoA-I has yet to be elucidated. There are two prevailing hypotheses describing the interaction. First, several investigators have argued that a direct protein-protein binding event occurs between apoA-I and the ABCA1 transporter (15, 19). Wang *et al.* (15) have shown, as have several other groups (15, 16, 19), that apoA-I and ABCA1 can be chemically cross-linked, strongly supporting a close and sustained proximity between the two molecules at the cell surface. However, numerous studies have shown that a majority of the plasma apolipoproteins containing lipophilic class A amphipathic helices can promote lipid efflux (4, 17, 20), as can multiple amphipathic helical peptides (3, 4) and even apolipophorins from insects (20). The lack of an obvious common binding sequence among these apolipoproteins has cast doubt on the idea of a highly specific interaction with ABCA1. In light of these studies, a second hypothesis has been proposed suggesting an interaction between apoA-I and lipid domains in the cell membrane formed by ABCA1, a suspected membrane lipid

* This work was supported by NHLBI, National Institutes of Health Grant RO1 HL62542 (to W. S. D.) and a summer graduate student fellowship from the University of Cincinnati Research Counsel (to S. E. P.). The costs of publication of this article were defrayed in part by the payment of page charges. This article must therefore be hereby marked "*advertisement*" in accordance with 18 U.S.C. Section 1734 solely to indicate this fact.

‡ Established Investigator of the American Heart Association. To whom correspondence should be addressed: Dept. of Pathology and Laboratory Medicine, Univ. of Cincinnati, 231 Albert Sabin Way, Cincinnati, OH 45267-0529. Tel.: 513-558-3707; Fax: 513-558-2289; E-mail: Sean.Davidson@UC.edu.

[1] The abbreviations used are: HDL, high density lipoprotein; ABCA1, ATP-binding cassette A1; apo, apolipoprotein; BSA, bovine serum albumin; DMPC, 1,2-dimyristoyl-sn-glycero-3-phosphatidylcholine; rHDL, reconstituted HDL; DMEM, Dulbecco's modified Eagle medium; WT, wild type.

translocase (5, 21). This view gained support from studies showing that an intact ABCA1 ATPase activity was required for apoA-I binding to the cell surface (21). In addition, several of the studies on non-apoA-I acceptors have shown a strong correlation between lipid binding affinity/helical content *versus* measured apolipoprotein-mediated lipid efflux (3, 4, 17, 20).

Knowledge of the necessary regions of apoA-I and the characteristics that make them critical for the interaction would provide valuable information on the mechanism of ABCA1-mediated lipid efflux. Two previous studies have used deletion mutants to suggest that the extreme C terminus of apoA-I is required for lipid efflux via this mechanism in human fibroblasts (5, 22) and THP1 macrophages (5). However, the deletion of a large region of apoA-I could be envisioned to have profound effects on long range structural interactions within the tertiary structure of the free protein, *i.e.* the structure of some other active region of the protein could have been perturbed. In addition, the C terminus of apoA-I is well known to be responsible for lipid binding (23–25). Because the ultimate product of apolipoprotein-mediated cholesterol efflux is a lipidated form of apoA-I, it is perhaps not surprising that a protein lacking its best lipid-binding region did not perform well in the assay.

To further study this question, we employed three mutagenesis strategies. First, we performed deletion mutagenesis to confirm the results from the studies mentioned above. Second, we followed up these studies with subtle point mutagenesis in the active region to reduce the likelihood of large changes in protein structure. Finally, we made "helix swap" mutants in which one helix of apoA-I was replaced with another to maintain protein length and number of helical domains. We found that helix 10 of apoA-I is critical for ABCA1-mediated cholesterol efflux from RAW macrophages and that its unique charge characteristics are critical in this role. Furthermore, we show that the lipid affinity of mutants containing helix 10 mutations correlates positively with lipid release from cells. However, we found no such correlation when other areas of the protein were mutated as long as an intact helix 10 was present at the C terminus. From these observations, we propose a new model for the apoA-I/ABCA1 interaction that we believe fits the majority of the available data.

EXPERIMENTAL PROCEDURES

Materials

IgA protease was purchased from Mobitech (Marco Island, FL). BL-21(DE3) *Escherichia coli* and the pET30 vector were from Novagen (Madison, WI). Isopropyl-β-D-thiogalactoside was from Fisher. 1-Palmitoyl, 2-oleoyl phosphatidylcholine and 1,2-dimyristoyl-sn-glycero-3-phosphatidylcholine (DMPC) were acquired from Avanti Polar Lipids (Birmingham, AL). Fatty acid-free bovine serum albumin (BSA) was from Calbiochem (San Diego, CA). 8-Bromoadenosine 3′:5′-cAMP was from Sigma. Fetal bovine serum and phosphate-buffered saline were from Invitrogen. RAW 264.7 mouse macrophage cells were from American Type Culture Collection (Manassas, VA). All chemical reagents were of the highest quality available.

Methods

Construction of Expression Vectors for Mutant Forms of ApoA-I—The manipulations to the DNA sequence of the apoA-I cDNA were accomplished in the pET30 vector using standard PCR techniques. The construct contained a histidine tag sequence with an IgA protease cleavage site (for a detailed description of the protein expression and purification protocol see Ref. 26). For the mutant Δ1–43, the forward primer[2] included a clamp region complimentary to helix 1 of the gene (as numbered by Roberts *et al.* (27)), a flap region with the sequence for an IgA protease cleavage site, and an *Nco*I cleavage site for ligation of the PCR product into the pET30 expression vector. The reverse primer was the M13 reverse primer. The H4@H1 mutant was created in a similar fashion. Note: the HX@HY notation refers to the replacement of the sequence for helix X with the sequence for helix Y (see Fig. 3). The H1@H10 mutant was designed with a clamp region complimentary to helix 9 and a flap region with the sequence of helix 1; this primer was the antisense primer, and the T7 promoter primer was the forward primer. The H10@H7 and was made by inserting a PCR-amplified product of helix 10 into the new location, using the Fsp1 and Nar I sites. Δ165–220 was created by simply placing a stop codon after the first repeat of helix 10 in the H10@H7 construct. For the latter mutants, PCR amplification was carried out using a Perkin Elmer thermocycler: 1 min hold at 94 °C; 30 rounds of 94 °C for 1.5 min, 55 °C for 1.5 min, 72 °C for 1.5 min; followed by a hold for 10 min at 72 °C to ensure full extension. Platinum *Pfx* polymerase (Invitrogen) was utilized for the reactions. The PCR product was cut with *Nco*I (New England Biolabs, Beverly, MA) and *Hin*dIII (Invitrogen) and ligated into the pET30 vector cut with the same enzymes. The sequence of each construct was verified on an Applied Biotechnology System DNA sequencer at the University of Cincinnati DNA core. PCR-based site-directed mutagenesis (QuikChange, Novagen, Madison, WI) was utilized to make the point mutations in apoA-I. The PCR was performed directly in the pET30 vector (94 °C, 1 min; 18 cycles of 94 °C, 1 min, 72 °C 1 min, 68 °C 10 min; followed by an additional 10 min at 68 °C to assure full extension). Site-directed mutagenesis was also used to create the C-terminal truncation mutants by adding a stop codon at the indicated location.

Protein Expression and Purification—The pET30 vectors containing the mutant apoA-I constructs were transfected into BL-21 *E. coli* cells, expressed, and purified according to established methods (26).

Cholesterol Efflux Studies—The transformed mouse macrophage cell line RAW264.7 (American Type Culture Collection) was maintained in Dulbecco's modified Eagle medium (DMEM, Invitrogen) with 10% fetal bovine serum and 50 μg/ml gentamycin. The cells were grown to 75% of confluence in a 48-well plate, then growth medium was removed, and [^{3}H]cholesterol labeling medium was added for 24 h (DMEM, 10% fetal bovine serum, 50 μg/ml gentamycin, 1.0 μCi/ml [^{3}H]cholesterol (Amersham Biosciences); 0.5 ml/well). After 24 h, the labeling medium was removed, and the cells were washed twice with phosphate-buffered saline (Invitrogen) containing 0.2% BSA and once with DMEM containing 0.2% BSA. Efflux medium was added (DMEM, 0.2% BSA, 10 μg/ml acceptor (apoA-I or specified mutant), with or with out 0.3 mM cAMP). A 100-μl sample of efflux medium was removed after 24 h and filtered through a 0.45-μm filter to remove any floating cells. The amount of [^{3}H]cholesterol in the medium was then measured by liquid scintillation counting. The percentage of efflux was calculated by dividing the counts in the medium by total counts in the cells at time 0 (28).

DMPC Clearance—DMPC in chloroform (Avanti Polar Lipids) was dried in a glass tube and brought up in 1 ml of standard Tris buffer at a concentration of 5 mg/ml. Multilamellar liposomes were formed by sonication for 30 s with a model 550 sonic dismembrator at level 5 with a microtip (Fisher). The experiments were performed in a Amersham Biosciences Ultraspec 4000 at a constant temperature of 25 °C, as maintained by circulating water bath, by adding the acceptor apolipoproteins to the liposomes (in standard Tris buffer) at a mass ratio of 2.5:1 (DMPC:protein). The change in light scattering was recorded over 30 min at 325 nm. The curves were normalized by calculating the percentage of turbidity clearance as a percentage of original light scatter at T_0 (before lipid-free acceptor was added). The rates were calculated for the first 5 min of the assay. The data were fit to a single exponential decay curve as a function of time (t): $f(t) = a^{-kt}$ using Sigma Plot 2000 (29).

Preparation of rHDL Particles—rHDL particles were prepared using 1-palmitoyl 2-oleoyl phosphatidylcholine (Avanti Polar Lipids, Alabaster, AL) at lipid to protein molar ratios of 110:1 according to the method of Jonas (30). The lipids were dried under nitrogen and resuspended in Tris salt buffer. Deoxycholate (1.3:1, w/w, deoxycholate:lipid) was added and incubated at 37 °C for 1.5 h with mild vortexing every 15 min. The protein was then added and incubated a 37 °C for 1 h. The cholate was dialyzed against standard Tris buffer (five changes of 2 liters). The particles were analyzed on a nondenaturing, native polyacrylamide gel using the Phast gel electrophoresis system (Amersham Biosciences) (31).

Circular Dichroism—The samples were diluted to 0.1 mg/ml on 20 mM phosphate buffer. The spectra were taken in a Jasco S-720 spectropolarimeter using a 0.1-cm path-length quartz cuvette. The spectra were accumulated over wavelengths of 250–185 nm. The percentage of α-helix was calculated from mean residual ellipticity at λ = 222 nm (32). For guanidine denaturation studies, the samples were prepared at 0.1 mg/ml in 20 mM phosphate buffer (pH 7.8) with increasing amounts of guanidine (ranging from 0 to 5.85 M) for guanidine denaturation curves and incubated for 3 days at 4 °C (33).

[2] For primer information please contact the corresponding author.

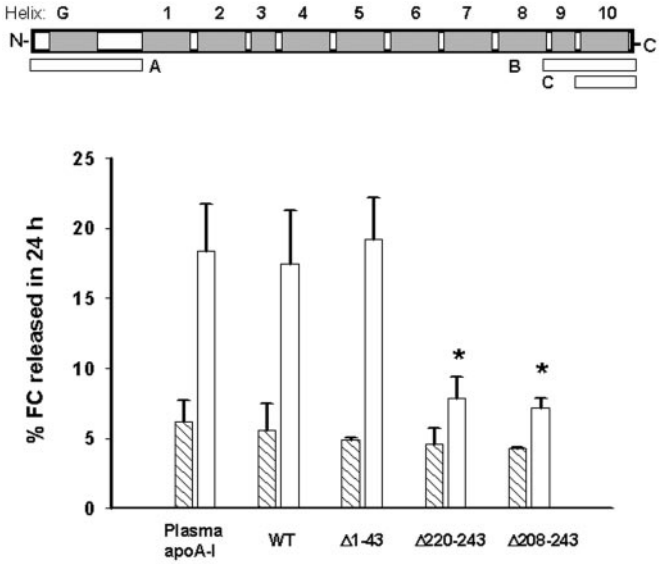

FIG. 1. **Apolipoprotein-mediated cholesterol efflux from RAW264 macrophages to deletion mutants of apoA-I.** RAW264 cells were labeled for 24 h with [^{3}H]cholesterol as described under "Experimental Procedures." After three washes, DMEM with 0.2% BSA containing 10 μg/ml of lipid-free acceptor protein ± 0.3 mM 8-bromo-cAMP was added to the cells for 24 h. The *hatched bars* represent samples without cAMP, whereas the *white bars* are samples with cAMP treatment. The protein regions missing in each deletion mutant are indicated by the *lettered bars* under the linear diagram of apoA-I, where *gray boxes* represent each putative helix, as represented originally by Roberts *et al.* (27): *Box A*, deletion of the N-terminal globular domain (Δ1–43); *box B*, deletion of the 9th and 10th helices of apoA-I (Δ208–243); *box C*, deletion of helix 10 (Δ220–243). The efflux data are expressed as percentages of total cell cholesterol for cells whose lipids were extracted immediately after the washes that followed labeling. The *error bars* represent the S.D. of data averaged from three separate experiments each performed in triplicate. A one-way analysis of variance followed by a Tukey post hoc test was performed to determine significant differences in efflux from wild type apoA-I: *, $p < 0.05$. *FC*, free cholesterol.

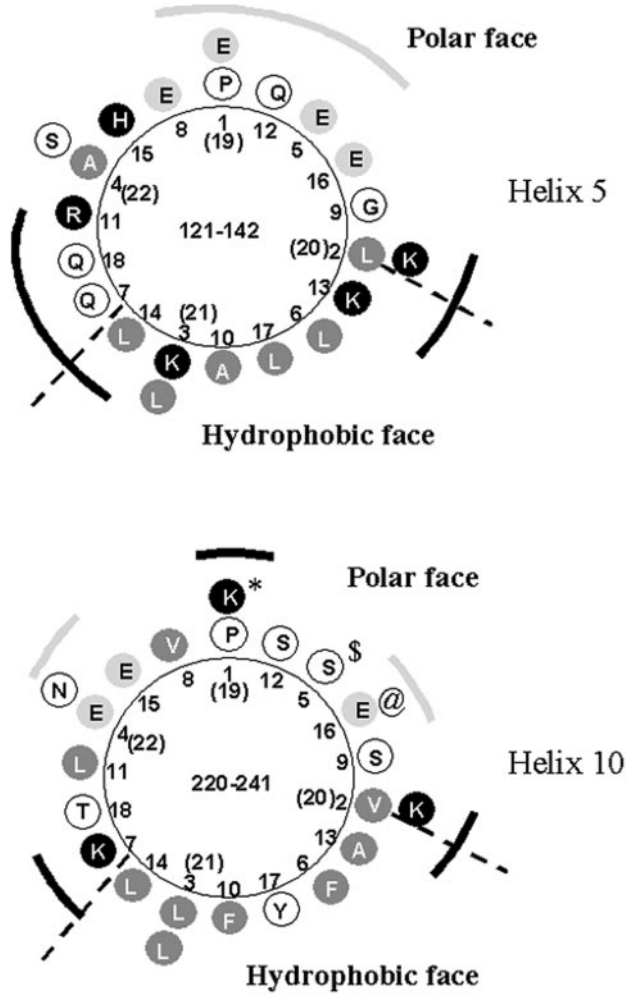

FIG. 2. **Edmundson helical wheel diagrams showing locations where mutations were made to perturb the charge distribution in helix 10.** These diagrams represent a view down the long axis of the α-helix and show the charge distributions on the polar and hydrophobic faces of apoA-I helix 10 (*bottom*). Helix 5 (*top*) is shown as an example of a class A helix representing a majority of the 22-amino acid helices in apoA-I (helices 1, 2, and 5–8) where helix 10 is a class Y helix (39). The amino acids in *white letters* within the *black circles* are positively charged; the amino acids in *black letters* in the *light gray circles* are negatively charged; amino acids in *white circles* are neutrally charged; amino acids in *white letters* in the *dark gray circles* are hydrophobic. The *thick dashed lines* delineate the hydrophobic face from the polar face. The *black solid lines* represent the positively charged regions of the polar face, and the *light gray solid lines* show the negatively charged regions of the polar face. The *symbols* represent amino acids where charge mutations were made: *, K238E; $, S224D; @, E235K.

RESULTS

We chose the RAW 264 mouse macrophage cell line for these studies because ABCA1 is up-regulated in both message and protein by incubation with cAMP analogs. This has been well documented by others (16, 18, 34) as well as confirmed in our lab (data not shown). This system is well suited to our study because the ability of the various mutants to promote cholesterol efflux could be compared in the presence or comparative absence of ABCA1 by incubating with or without the cAMP analog.

Truncation Mutants—We made two deletions in the C terminus of human apoA-I by inserting stop codons at amino acids 220 and 208. We also deleted the N-terminal 43 amino acids, which likely exist in a globular conformation (35) and have not been implicated in cholesterol efflux as a positive control for the deletion process (Fig. 1, *top panel*). The ABCA1-mediated efflux (Fig. 1, *open bars*) is distinguished from nonspecific levels of cholesterol efflux by comparison with samples without the cAMP analog (Fig. 1, *hatched bars*). Importantly, plasma apoA-I and our recombinant wild type apoA-I (WT) exhibited similar abilities to promote apolipoprotein-mediated cholesterol efflux, demonstrating that the recombinant protein was fully functional in this assay (26). The removal of the N-terminal 43 amino acids did not perturb apolipoprotein-mediated cholesterol efflux. However, the C-terminal truncations within apoA-I mutants reduced ABCA1-mediated cholesterol efflux nearly to background levels. This confirms studies in other cell types (5, 22) and suggests that apoA-I helix 10 is important to apolipoprotein-mediated cholesterol efflux.

Point Mutants—We used site-directed mutagenesis to make more subtle point mutants that perturbed charge on the polar face of helix 10. The polar face was targeted because our experience indicated that changes in this region are less likely to perturb the overall structure of the lipid-free protein than those targeting the nonpolar face (data not shown). We selected sites for mutation based on the unique properties of helix 10 *versus* the other 22-amino acid helices within apoA-I (Fig. 2; see "Discussion"). The following point mutants were generated: the positively charged Lys at position 238 (Fig. 2, *, K238E) was changed to negatively charged Glu. This change occurs at helical wheel position 19 (when Pro^{220} is considered the 1 position) in helix 10 and changes the class Y character of the helix to more like the class A helices in the protein. The neutrally charged Ser at position 224 (Fig. 2, $, S224D) was changed to a negatively charged Asp because this position (helical wheel

position 5) contains an acidic residue in every other 22-amino acid helix of apoA-I. Additionally, a negatively charged Glu at position 235, near the edge of the polar face at helical wheel position 16, was changed to a positively charged Lys (Fig. 2, @, E235K), to further change the charge distributions. Circular dichroism spectroscopy was performed to analyze the effects of the mutations on the total secondary structure of the protein. The average helical content for S224D, E235K, and the WT protein in the lipid-free form was 53 ± 5%, with no major differences apparent among them, indicating that the charge mutations did not have a major effect on the secondary structural content of the protein. This observation was not surprising because we have previously shown that the C terminus does not contribute substantial helicity to the protein in the lipid free state (24). K238E consistently exhibited a slightly lower helical content of about 48%, indicating that this change may have had a slight effect on the secondary structure of the protein. In addition, all three mutants exhibited similar free energies of denaturation (all three proteins averaged together of 3.1 kcal/mol ± 0.5) to the WT protein (2.8 kcal/mol ± 0.2) and human plasma apoA-I (2.9 kcal/mol ± 0.3). All three mutants formed rHDL particles of similar diameter as the WT protein when reconstituted with 1-palmitoyl 2-oleoyl phosphatidylcholine at a molar ratio of phospholipid to protein of 110:1, indicating that there were no major defects in these proteins in terms of forming stable HDL particles (data not shown).

Fig. 3 shows that the S224D and the K238E mutants exhibited reduced levels of apolipoprotein-mediated cholesterol efflux relative to WT, whereas the E235K mutant was slightly more effective than WT. The differences in ABCA1-mediated cholesterol efflux persisted over a range of concentrations (Fig. 3*B*) where maximal levels of efflux were attained at around 20 μg/ml as previously reported (36). Although the S224D and the K238E mutants showed reduced levels of apolipoprotein-mediated efflux relative to WT, both were more effective than the Δ220–243 mutant (Fig. 1).

Because the lipid binding characteristics of apoA-I have been proposed to be important in the ABCA1/apoA-I interaction (5) and helix 10 is the strongest lipid binding helix in the protein (37), the abilities of the point mutants to interact with DMPC liposomes was assessed. Plasma apoA-I was previously shown to clear liposomes as well as the WT apoA-I (26). Fig. 3*C* shows that the S224D and K238E mutants exhibited a reduced ability to reorganize DMPC relative to WT apoA-I. Conversely, the E235K mutant exhibited a comparable efficiency to WT protein. Initial rates for these reactions are compared in Table I.

Helix Translocation Mutants—It is clear from Fig. 3 that the two point mutants that exhibited reduced levels of cholesterol efflux relative to WT also exhibited reduced lipid association characteristics. This suggests that the lipid affinity of helix 10 might be the important feature in the promotion of apolipoprotein-mediated cholesterol efflux. To further study this relationship, we performed a series of helix translocation mutants or helix swaps. We first replaced helix 10 with the sequence for helix 1 (H1@H10; Fig. 4). Helix 1 was selected for the replacement because, in peptide studies, its lipid binding properties have been shown to be most comparable with those of helix 10 (37). The mutant also exhibited an average helical content measured by CD that was comparable with but slightly lower than the WT apoA-I (44% *versus* 53%). Its free energy of denaturation was similar (3.2 ± 0.3 kcal/mol *versus* 2.8 ± 0.2 for WT), and it could be reconstituted into rHDL particles of similar size by the cholate dialysis technique (not shown). Fig. 5*A* shows that the H1@H10 mutant promoted cholesterol efflux at levels lower than WT but not as low as the mutant Δ220–243.

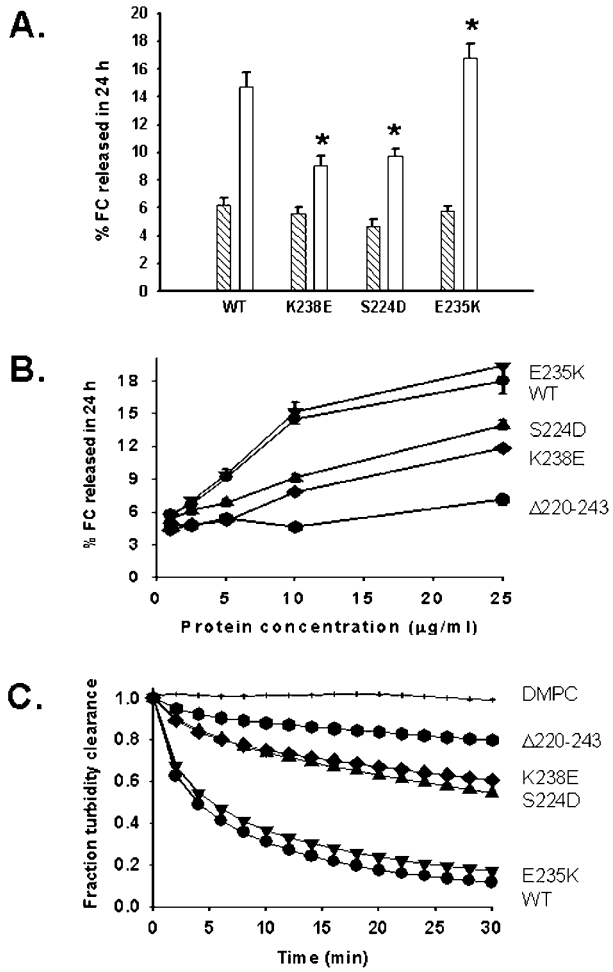

FIG. 3. **Effects of helix 10 point mutations on cholesterol efflux and DMPC clearance.** *A*, 24-h levels of cholesterol efflux. RAW264 cells were labeled and washed as described in the legend to Fig. 1. The *hatched bars* represent samples without cAMP, whereas the *white bars* indicate samples with 0.3 mM cAMP. The averaged data from two separate experiments each done in triplicate are shown ± S.D. The *asterisk* indicates significant difference from WT ($p < 0.05$) by analysis of variance. *B*, concentration dependence of efflux for each acceptor. The experimental conditions are identical to those described for Fig. 1 except the concentration of the acceptor protein was varied as shown. WT (*filled circles*) and Δ220–243 (*filled hexagons*) served as controls for normal and low levels of efflux, respectively. The point mutants are represented by the following *symbols*: ▲, S224D; ▼, E235K; ♦, K238E. The figure shows data from one experiment performed in triplicate ± S.D. *C*, kinetics of interaction of helix 10 point mutants with DMPC liposomes. Multilamellar DMPC liposomes suspended in standard Tris buffer were added to protein in a 2.5:1 mass ratio of DMPC:protein. Absorbance at 325 nm was recorded as a function of time for 30 min at a constant temperature of 24.5 °C as maintained by circulating water bath. Light scatter at 325 nm is expressed as a percentage of light scatter at $T = 0$ min (before apolipoprotein was added) and reflects the ability of a particular point mutant to rearrange lipids into small discs. Each protein is represented by the same symbols indicated in *B*. The *DMPC curve* represents levels of light scatter with addition of appropriate amount of buffer without apolipoprotein. Each curve represents the average of at least three separate experiments performed on the same day with the same preparations of protein that were used for the cholesterol efflux determinations. *FC*, free cholesterol.

The H1@H10 mutant also exhibited a reduced rate of lipid clearance relative to WT apoA-I (Fig. 5*B* and Table II).

To determine whether helix 10 could confer efficient efflux capabilities on forms of apoA-I that had been modified in regions outside of helix 10, we generated three additional mutants (Fig. 4). To see whether protein length was an important factor, we made an internal deletion of amino acids 165–220, which removed helices 7 and 8 but kept an intact helix 10 on

TABLE I
Rate constants of helix 10 point mutants and controls for DMPC clearance assay

	k^a
Plasma apoA-I	0.13 ± 0.02
Wild type	0.14 ± 0.04
S224D	0.04 ± 0.01
E235K	0.14 ± 0.01
K238E	0.04 ± 0.01
Δ220–243	0.017 ± 0.01

[a] The *k* value represents the rate constant derived from the first 5 min of the DMPC clearance (see "Methods").

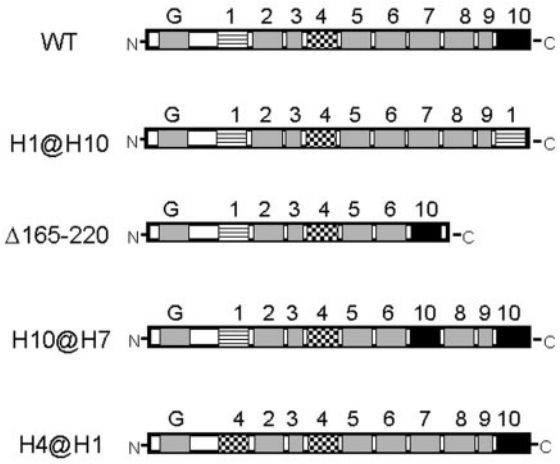

FIG. 4. **Linear diagrams of helix translocation mutants.** Each *shaded box* represents either a 11- or 22-mer amphipathic α-helix of apoA-I. The *black boxes* represent the locations of the amino acid sequence of helix 10, the *horizontally striped boxes* represent the locations of the amino acid sequence of helix 1, and the *checkered boxes* show the locations of the amino acid sequence of helix 4. The *G* represents the helix in the N terminus that is predicted to be in globular structural motifs (39).

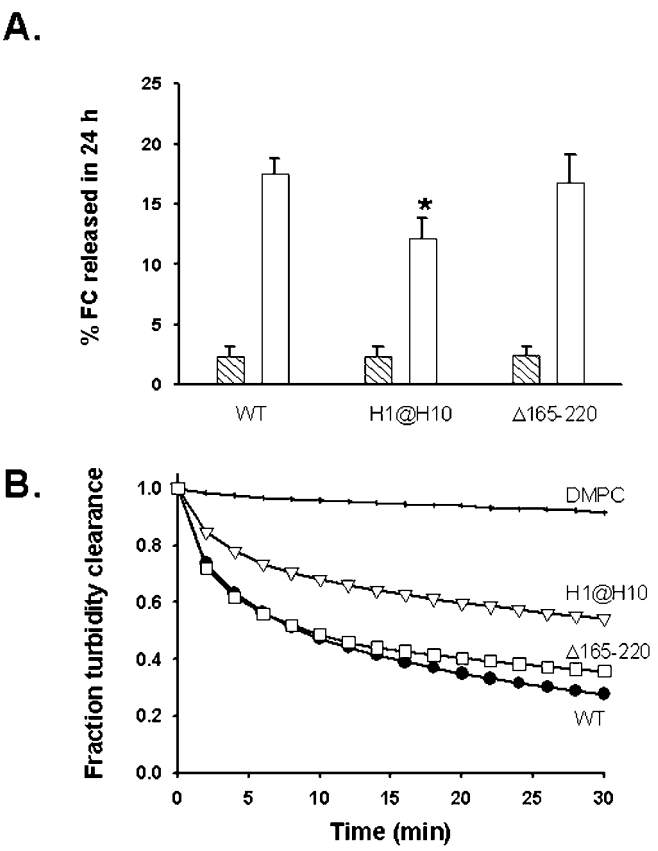

FIG. 5. **Analysis of the helix 10 translocation mutants.** *A*, apolipoprotein-mediated cholesterol efflux at 24 h. The experiment was performed as described for Fig. 1. The *hatched bars* represent samples without cAMP, whereas the *white bars* indicate samples with 0.3 mM cAMP. The data shown are the averages of two separate experiments performed in triplicate ± S.D. The *asterisk* indicates significant difference from WT ($p < 0.05$) by analysis of variance. *B*, DMPC clearance ability: The experiments were performed as in Fig. 3. The *symbols* are: ●, WT apoA-I; ▽, H1@H10; □, Δ165–220. The *curves* represent averages of at least four experiments. *FC*, free cholesterol.

TABLE II
Rate constants of the helix translocation mutants for DMPC clearance assay

	k^a
Wild type	0.14 ± 0.04
Δ165–220	0.11 ± 0.01
H1@H10	0.05 ± 0.01
H10@H7	0.04 ± 0.01
H4@H1	0.06 ± 0.01

[a] The *k* value represents the rate constant derived from the first 5 min of the DMPC clearance (see "Methods").

the C terminus. The Δ165–220 mutant was less helical (about 45% *versus* 53% for WT) and made smaller rHDL discs than did the WT (not shown) as expected from the reduction in helical domains (38). Fig. 5 shows that the Δ165–220 mutant was equal to WT in both the cholesterol efflux and DMPC clearance assays. This suggests that as long as an intact helix 10 domain is present at the C terminus, even substantial deletions of the rest of the protein do not effect lipid transfer. This agrees with work published by Burgess *et al.* (22), in which they showed that deletions in the central region of apoA-I (Δ100–143, Δ122–165, and Δ144–186) also had little effect on apolipoprotein-mediated efflux from THP1 macrophages.

To determine whether an additional copy of helix 10 within the sequence might confer additional cholesterol efflux capabilities upon apoA-I, the mutant H10@H7 was constructed. Finally, we generated an additional mutant, H4@H1, which had the putative high lipid affinity helix 1 replaced with a second copy of a lower lipid affinity helix 4 (37) but still had helix 10 in its normal location at the C terminus. Both of the full-length mutants exhibited α-helical contents, free energies of denaturation, and ability to form rHDL particle diameters similar to the WT apoA-I (data not shown). The ability of these helix translocation mutants to promote cholesterol release from RAW264 macrophages and to interact with DMPC liposomes is shown in Fig. 6. Both mutants H10@H7 and H4@H1 exhibited cholesterol efflux capabilities similar to WT (Fig. 6*A*), even across various concentrations of acceptor (Fig. 6*B*). However, we were surprised to find that they also exhibited markedly reduced lipid association characteristics with the liposomes. These two mutants were different from all other mutants in this study in that their lipid association characteristics did not correlate with their ability to promote cholesterol release. This point is illustrated in Fig. 7, which plots the initial rates of DMPC clearance with the hourly rate of cholesterol efflux (calculated by simply dividing the total percentage of released cholesterol from RAW cells over a 24-h incubation at 10 μg/ml). All of the mutants that had mutations affecting the sequence of helix 10 fell on a straight line with a correlation coefficient of 0.927. We found a similar correlation regardless of the apoA-I concentration used (as long as it was significantly below the saturation level of around 20 μg/ml) and at shorter incubation times. However, the mutants that contained helix translocations in regions outside of helix 10 did not fall on the line. These points are shown superimposed on the plot in Fig. 7 for demonstration purposes and are not part of the regression line. The

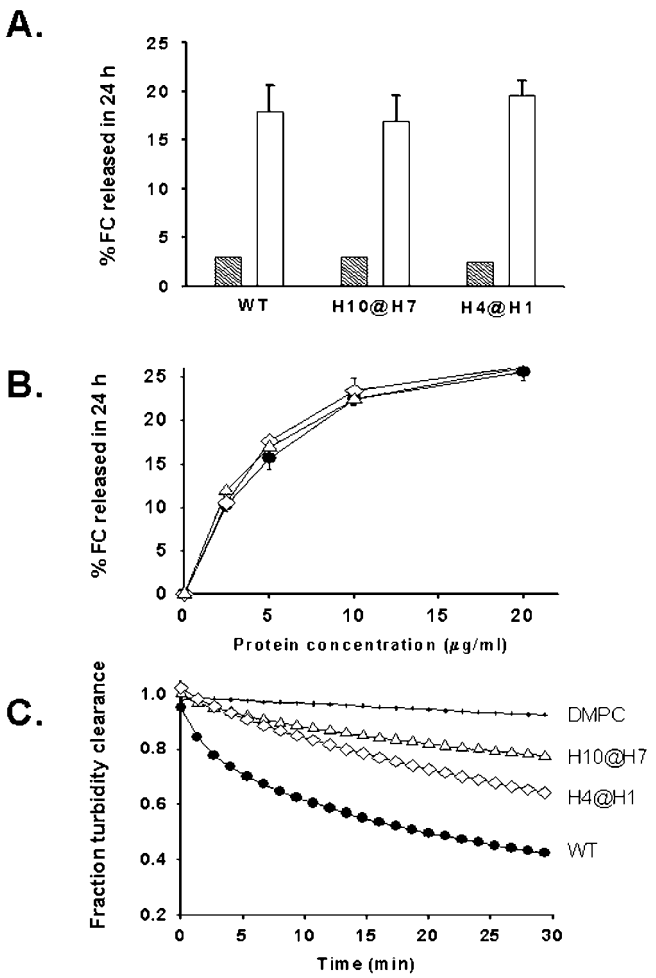

FIG. 6. **Analysis of helix translocation mutants containing helix translocation mutations that do not affect the sequence or position of helix 10.** *A*, cholesterol efflux at 24 h. These experiments were performed as described for Fig. 1. The *hatched bars* represent samples without cAMP, whereas the *white bars* indicate samples with 0.3 mM cAMP. The results are averaged from two experiments each performed in triplicate ± S.D. *B*, concentration dependence of efflux for each acceptor: These experiments were performed as in Fig. 1 except that the amount of acceptor lipid-free protein was varied as indicated. The results are from one experiment performed in triplicate ± S.D. The *symbols* are: ●, WT; ◇, H10@H7; △, H4@H1. *C*, DMPC clearance ability. These experiments were performed as for Fig. 3. The *symbols* are the same as in B. Each curve is an average of three separate experiments. *FC*, free cholesterol.

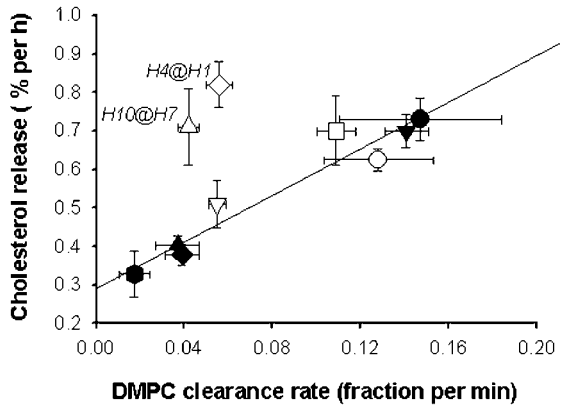

FIG. 7. **Plot of cholesterol release from RAW macrophages as a function of initial rates of DMPC clearance for all mutants of apoA-I used in this study.** The rate of DMPC clearance (*k*) (see "Methods") for the first 5 min of the assay (Tables I and II) is plotted against percentage of cholesterol release/h for all mutants tested in this study. The cholesterol release was calculated by dividing the percentage of cholesterol efflux over a 24-h incubation using 10 μg/ml of apoA-I or mutant. The *symbols* are: ○, plasma apoA-I; ●, WT apoA-I; ▲, S224D; ▼, E235K; ♦, K238E; ▽, H1@H10; □, Δ165–220; ◇, H10@H7; △, H4@H1. A best fit regression line was plotted through the following data points: plasma apoA-I, WT, S224D, E235K, K238E, H1@H10, Δ165–220, and Δ220–243 (R^2 = 0.927). The H4@H1 and H10@H7 were not included in the regression and are labeled to highlight the fact that they do not fit on the line. The data points are the averages of data from a minimum of two experiments ± S.D. on each axis.

data can be summarized by stating that as long as there was an intact helix 10 sequence at the C terminus of an apoA-I mutant, cholesterol efflux was maintained at levels equal to WT apoA-I. Conversely, whenever we mutated or deleted the helix 10 sequence, cholesterol efflux was perturbed.

DISCUSSION

This study resulted in two important observations pertaining to the mechanism of apoA-I-mediated cholesterol efflux from macrophages. First, we have demonstrated that helix 10 (residues 220–243), because of its unique charge distribution, is critical for promotion of optimal lipid efflux via the ABCA1 pathway. Second, we found that the correlation between lipid binding and ABCA1-mediated efflux noted for changes in the helix 10 region does not hold when other regions of the protein are mutated, as long as there is a functional helix 10 at its native location at the C terminus. We discuss the implications of these findings below in terms of the structure of apoA-I and the mechanism of the apoA-I/ABCA1 interaction.

The Structure of ApoA-I Helix 10—ApoA-I contains two major types of amphipathic α-helices defined by the arrangement of positively and negatively charged amino acids on the helical polar face (reviewed in Ref. 39). When it was clear from our cholesterol efflux experiments that mutants lacking helix 10 were poor acceptors of cellular lipids, we studied the properties of this helix *versus* the others in the protein. Helix 10 is distinguished from the majority of helices within apoA-I in that it is not a typical class A helix. Class A helices (helices 1, 2, and 5–8) have positively charged amino acids surrounding the nonpolar face with negatively charged amino acids clustered at the center of the polar face. Class Y helices (helices 4 and 10) are organized similarly but have a positive charge disrupting the cluster of negative charges on the polar face. The Edmundson helical wheel diagrams in Fig. 2 illustrate the polar face differences in helix 10 *versus* a class A helix represented by helix 5. In helix 10, the positive charge of the lysine at amino acid 238 interrupts the loose cluster of negative charges on the top of the polar face (see the *asterisk*). In many other helices of apoA-I (helices 1, 5, 7, and 8), this position contains an acidic residue. In addition, the serine at amino acid 224 (position 5 in the helical wheel) is unique to helix 10; all of the other helices in the protein contain an acidic residue at this location. When we reversed the charge at amino acid 238 and placed a negative charge at amino acid 224, apoA-I exhibited a decreased ability to promote cholesterol efflux in our assay. However, when we targeted glutamate 235, which occurs at position 16 in helix 10, we saw no decline and even a slight increase in cholesterol efflux. The amino acids at position 16 in the helices of apoA-I are not highly conserved and can have acidic, basic, neutral, and even hydrophobic residues at this position. Importantly, we noticed that the same mutants that exhibited reduced cholesterol efflux ability also exhibited reduced ability to associate with DMPC liposomes. This strong correlation between the lipid binding ability of a given mutant and its ability to promote receptor-mediated efflux was also evident when helix 10 was replaced with the second strongest lipid binding helix 1 (H1@H10) (37). Therefore, the unique charge distribution on

the polar face of helix 10 is an important factor for maximal lipid binding and promotion of ABCA1-mediated cholesterol efflux. This agrees with previous studies that show that helix 10 exhibits unique physical properties (helical wedge angle, hydrophobic moment, etc.) that allow it to efficiently associate with lipids (37), and it is well known from experimental and theoretical analyses of amphipathic helices that differences in the charge distribution of the polar face can have significant effects on lipid binding (40).

Our data also indicate that as long as there is a functional helix 10 at the C terminus of apoA-I, the length of the protein is not critical to cholesterol efflux, because the Δ208–243 and Δ220–243 truncation mutants are not functional, whereas adding helix 10 to the end of a truncated mutant salvages activity (Δ165–220) (22). In addition, the mutant H4@H1, which lacks the other strong lipid binding helix (helix 1) and subsequently has reduced lipid affinity, still promotes efflux at levels similar to WT protein. Similarly, the mutant H10@H7 containing two copies of helix 10, with one copy in the native location, also promotes efflux at normal levels. Together these data indicate that the presence of helix 10 at the C terminus, with its specific charge distribution, is critical to apolipoprotein-mediated cholesterol efflux.

The Role of Lipid Binding Affinity in Apolipoprotein-mediated Cholesterol Efflux—The striking correlation shown in Fig. 7 for apoA-I mutants, in which helix 10 has been modified, strongly suggests that this region of apoA-I plays a significant role in a lipid binding step occurring at some point during the lipid transfer process. As discussed in the Introduction, the hypothesis of a lipid/protein interaction predicts that apoA-I initiates lipid transfer by binding to a localized, preformed lipid domain resulting from the ATPase driven activity of ABCA1 (21). The identity and/or composition of this domain has been suggested to be due to ABCA1-driven translocation of phosphatidylserine to the outer monolayer of the membrane (21); however, this remains controversial (41). The presence of the modified lipid domain may destabilize the outer leaflet facilitating the insertion of apoA-I helices, thus allowing it to "microsolubilize" a patch of membrane and leave as a nascent HDL particle (42). This view has been supported by observations that a functional ATPase (and hence, the floppase activity) is required for apoA-I binding to cell surfaces (21). In fact, two groups have shown marked membrane structure perturbations in ABCA1 expressing cells (15, 43).

However, the current study also demonstrated the important result that apoA-I mutants with sequence changes in locations that do not alter the sequence or location of helix 10 can have profound effects on DMPC clearance without affecting apolipoprotein-mediated lipid release. To our knowledge, this is the first time a mutant of apoA-I has been described with such a disparity between these two activities. We believe this indicates that the mechanism for apoA-I solubilization of lipids at the surface of a DMPC liposome is very different from that occurring near ABCA1 in the membrane. The clearance of DMPC liposomes is likely a multistep process that involves an initial interfacial binding step (perhaps mediated by helix 10) followed by a reorganization step that is driven by the lipid affinity and cooperative binding of all of the remaining helices in apoA-I (37). If one assumes a similar protein to lipid interaction at an ABCA1-generated cellular lipid domain, then H10@H7 and H4@H1, based on their lower DMPC clearance rates, would be expected to be defective in promoting cholesterol efflux. The fact that they performed as well as WT (Fig. 6) suggests that the rate of cellular lipid release is not solely dependent on the ability of apoA-I to reorganize an unstable ABCA1-generated lipid domain. Thus, we believe that our data argue against the idea that ABCA1 simply forms an unstable membrane domain that is subsequently solubilized by a detergent-like activity of apoA-I. It follows that the driving force for lipidation of apoA-I likely comes as a result of a much more active process.

Although our studies do not address the identity of this active process, other investigators have provided convincing evidence that apoA-I may directly interact with ABCA1 itself during the lipid transfer process. ApoA-I can be cross-linked to ABCAI (15, 16), and very recent studies by Fitzgerald *et al.* (19) have demonstrated that the extracellular loops between helices 1 and 2 and helices 7 and 8 of ABCA1 could be responsible for binding apoA-I. If this is the case, then our data suggest that the helix 10 region of apoA-I is an important participant in the interaction. This productive binding event could result in the lipidation of apoA-I by an ATP-driven lipid transfer mechanism mediated by ABCA1 that does not depend on the ability of apoA-I to solubilize a membrane surface. This scheme could account for the ability of H4@H1 and H10@H7 to promote cholesterol efflux, even though they cannot clear DMPC liposomes as effectively as WT.

However, the idea of a direct apoA-I to ABCA1 interaction is less satisfying in light of the strict correlation between lipid binding parameters and apolipoprotein-mediated cholesterol efflux when mutations are made in helix 10 of apoA-I. It is possible that the characteristics conferring excellent lipid affinity on a given amphipathic helix might also confer an enhanced ability to bind to the putative ABCA1-binding site. However, another possibility that seems more likely is that helix 10 may function to tether the lipid-free apoA-I to the ABCA1-generated lipid domain of the cell membrane in close proximity to ABCA1. The tethered apoA-I could then diffuse within the plane of the membrane until it comes in contact with ABCA1, where a productive protein/protein interaction could lead to the lipidation of apoA-I. After lipidation, a lipid-poor (pre-β) form of apoA-I is released from the membrane, possibly because of conformational changes in apoA-I resulting from lipid binding. This mechanism is similar to one proposed very recently by Burgess *et al.* (44) in which they suggest that phospholipid contained in the extracellular matrix of macrophages acts as an initial tether point for apoA-I, bringing it into close proximity to membrane-bound ABCA1.

Although admittedly speculative, we believe that our data support this hybrid model better than either the straight protein/protein or lipid interaction hypotheses alone. It explains the requirement for helix 10 in apoA-I and the correlation of the lipid association characteristics of helix 10 with lipid efflux. The lack of such a correlation when changes are made outside of helix 10 is explained by the idea that only helix 10 is required for the initial cell surface and/or extracellular matrix contact. Once apoA-I is tethered to the membrane, the well known low specificity of the apoA-I/ABCA1 interaction is not significantly affected by internal helix swapping mutations, so long as the protein is predominantly composed of amphipathic helices. We believe that this two-step model unifies much of the apparently conflicting data in the literature. For example, it provides a basis for the cross-linking of ABCA1 and apoA-I (15, 16) while still allowing for the observed correlations between lipid binding affinity and apolipoprotein-mediated cholesterol efflux (5). The presence of lipid associated forms of apoA-I as well as ABCA1-bound apoA-I populations may account for conflicting results from fluorescent measurements of apoA-I mobility on the cell surface (21, 41). In addition, Fitzgerald *et al.* (19) have suggested that the lack of measurable ABCA1/apoA-I cross-linking at low temperatures could be due to changes in membrane fluidity that affect the initial insertion of apoA-I into the

lipid bilayer, thereby preventing subsequent contact with ABCA1. It should be cautioned, however, that no data exist on the sequence of the helix 10 interaction *versus* lipidation events. For example, it is possible that apoA-I may interact with ABCA1 first, followed by contact with the membrane by helix 10. Clearly, more work is necessary to clarify the details of this mechanism.

Regardless of whether apoA-I helix 10 interacts with lipid or ABCA1 itself, it is likely that analogous functional regions exist in the other exchangeable apolipoproteins capable of apolipoprotein-mediated cholesterol efflux. Obviously, these regions must have different sequences than that found in helix 10 of apoA-I, but it is likely that more general characteristics such as helical charge distribution and lipid affinity of the active regions in these proteins will exhibit similarities. Indeed, the C-terminal regions of apoE, apoA-IV, and apoA-II are known to mediate lipid binding much like helix 10 of apoA-I. Truncation of the C-terminal region of apoE has already been shown to reduce phospholipid efflux (5). Future studies will be needed in full-length versions of these proteins to identify those regions that are critical to the interaction.

REFERENCES

1. Gordon, T., Castelli, W. P., Hjortland, M. C., Kannel, W. B., and Dawber, T. R. (1977) *Am. J. Med.* **62,** 707–714
2. Johnson, W. J., Mahlberg, F. H., Rothblat, G. H., and Phillips, M. C. (1991) *Biochim. Biophys. Acta* **1085,** 273–298
3. Mendez, A. J., Anantharamaiah, G. M., Segrest, J. P., and Oram, J. F. (1994) *J. Clin. Invest.* **94,** 1698–1705
4. Yancey, P. G., Bielicki, J. K., Johnson, W. J., Lund-Katz, S., Palgunachari, M. N., Anantharamaiah, G. M., Segrest, J. P., Phillips, M. C., and Rothblat, G. H. (1995) *Biochemistry* **34,** 7955–7965
5. Gillotte, K. L., Zaiou, M., Lund-Katz, S., Anantharamaiah, G. M., Holvoet, P., Dhoest, A., Palgunachari, M. N., Segrest, J. P., Weisgraber, K. H., Rothblat, G. H., and Phillips, M. C. (1999) *J. Biol. Chem.* **274,** 2021–2028
6. Hara, H., and Yokoyama, S. (1991) *J. Biol. Chem.* **266,** 3080–3086
7. Schaefer, E. J., Zech, L. A., Schwartz, D. E., and Brewer, H. B. (1980) *Ann. Intern. Med.* **93,** 261–266
8. Brooks-Wilson, A., Marcil, M., Clee, S. M., Zhang, L. H., Roomp, K., van Dam, M., Yu, L., Brewer, C., Collins, J. A., Molhuizen, H. O., Loubser, O., Ouelette, B. F., Fichter, K., Ashbourne-Excoffon, K. J., Sensen, C. W., Scherer, S., Mott, S., Denis, M., Martindale, D., Frohlich, J., Morgan, K., Koop, B., Pimstone, S., Kastelein, J. J., and Hayden, M. R. (1999) *Nat. Genet.* **22,** 336–345
9. Bodzioch, M., Orso, E., Klucken, J., Langmann, T., Bottcher, A., Diederich, W., Drobnik, W., Barlage, S., Buchler, C., Porsch-Ozcurumez, M., Kaminski, W. E., Hahmann, H. W., Oette, K., Rothe, G., Aslanidis, C., Lackner, K. J., and Schmitz, G. (1999) *Nat. Genet.* **22,** 347–351
10. Rust, S., Rosier, M., Funke, H., Real, J., Amoura, Z., Piette, J. C., Deleuze, J. F., Brewer, H. B., Duverger, N., Denefle, P., and Assmann, G. (1999) *Nat. Genet.* **22,** 352–355
11. Horowitz, B. S., Goldberg, I. J., Merab, J., Vanni, T. M., Ramakrishnan, R., and Ginsberg, H. N. (1993) *J. Clin. Invest.* **91,** 1743–1752
12. Bortnick, A. E., Rothblat, G. H., Stoudt, G., Hoppe, K. L., Royer, L. J., McNeish, J., and Francone, O. L. (2000) *J. Biol. Chem.* **275,** 28634–28640
13. Langmann, T., Klucken, J., Reil, M., Liebisch, G., Luciani, M. F., Chimini, G., Kaminski, W. E., and Schmitz, G. (1999) *Biochem. Biophys. Res. Commun.* **257,** 29–33
14. Lawn, R. M., Wade, D. P., Garvin, M. R., Wang, X., Schwartz, K., Porter, J. G., Seilhamer, J. J., Vaughan, A. M., and Oram, J. F. (1999) *J. Clin. Invest.* **104,** R25–R31
15. Wang, N., Silver, D. L., Costet, P., and Tall, A. R. (2000) *J. Biol. Chem.* **275,** 33053–33058
16. Oram, J. F., Lawn, R. M., Garvin, M. R., and Wade, D. P. (2000) *J. Biol. Chem.* **275,** 34508–34511
17. Remaley, A. T., Stonik, J. A., Demosky, S. J., Neufeld, E. B., Bocharov, A. V., Vishnyakova, T. G., Eggerman, T. L., Patterson, A. P., Duverger, N. J., Santamarina-Fojo, S., and Brewer, H. B., Jr. (2001) *Biochem. Biophys. Res. Commun.* **280,** 818–823
18. Smith, J. D., Miyata, M., Ginsberg, M., Grigaux, C., Shmookler, E., and Plump, A. S. (1996) *J. Biol. Chem.* **271,** 30647–30655
19. Fitzgerald, M. L., Morris, A. L., Rhee, J. S., Andersson, L. P., Mendez, A. J., and Freeman, M. W. (2002) *J. Biol. Chem.*
20. Hara, H., Komaba, A., and Yokoyama, S. (1992) *Lipids* **27,** 302–304
21. Chambenoit, O., Hamon, Y., Marguet, D., Rigneault, H., Rosseneu, M., and Chimini, G. (2001) *J. Biol. Chem.* **281,**
22. Burgess, J. W., Frank, P. G., Franklin, V., Liang, P., McManus, D. C., Desforges, M., Rassart, E., and Marcel, Y. L. (1999) *Biochemistry* **38,** 14524–14533
23. Minnich, A., Collet, X., Roghani, A., Cladaras, C., Hamilton, R. L., Fielding, C. J., and Zannis, V. I. (1992) *J. Biol. Chem.* **267,** 16553–16560
24. Davidson, W. S., Hazlett, T., Mantulin, W. W., and Jonas, A. (1996) *Proc. Natl. Acad. Sci. U. S. A.* **93,** 13605–13610
25. Ji, Y., and Jonas, A. (1995) *J. Biol. Chem.* **270,** 11290–11297
26. Panagotopulos, S. E., Witting, S. R., Horace, E. M., Nicholas, M. J., and Sean, D. W. (2002) *Protein Expression Purif.* **25,** 353–361
27. Roberts, L. M., Ray, M. J., Shih, T. W., Hayden, E., Reader, M. M., and Brouillette, C. G. (1997) *Biochemistry* **36,** 7615–7624
28. Davidson, W. S., Lund-Katz, S., Johnson, W. J., Anantharamaiah, G. M., Palgunachari, M. N., Segrest, J. P., Rothblat, G. H., and Phillips, M. C. (1994) *J. Biol. Chem.* **269,** 22975–22982
29. McLean, L. R., and Hagaman, K. A. (1993) *Biochim. Biophys. Acta* **1167,** 289–295
30. Jonas, A. (1986) *Methods Enzymol.* **128,** 553–582
31. Davidson, W. S., Gillotte, K. L., Lund-Katz, S., Johnson, W. J., Rothblat, G. H., and Phillips, M. C. (1995) *J. Biol. Chem.* **270,** 5882–5890
32. Chen, Y. H., Yang, J. T., and Martinez, H. M. (1972) *Biochemistry* **11,** 4120–4131
33. Sparks, D. L., Lund-Katz, S., and Phillips, M. C. (1992) *J. Biol. Chem.* **267,** 25839–25847
34. Abe-Dohmae, S., Suzuki, S., Wada, Y., Aburatani, H., Vance, D. E., and Yokoyama, S. (2000) *Biochemistry* **39,** 11092–11099
35. Rogers, D. P., Brouillette, C. G., Engler, J. A., Tendian, S. W., Roberts, L., Mishra, V. K., Anantharamaiah, G. M., Lund-Katz, S., Phillips, M. C., and Ray, M. J. (1997) *Biochemistry* **36,** 288–300
36. Sakr, S. W., Williams, D. L., Stoudt, G. W., Phillips, M. C., and Rothblat, G. H. (1999) *Biochim. Biophys. Acta* **1438,** 85–98
37. Palgunachari, M. N., Mishra, V. K., Lund-Katz, S., Phillips, M. C., Adeyeye, S. O., Alluri, S., Anantharamaiah, G. M., and Segrest, J. P. (1996) *Arterioscler. Thromb. Vasc. Biol.* **16,** 328–338
38. Frank, P. G., Bergeron, J., Emmanuel, F., Lavigne, J. P., Sparks, D. L., Denefle, P., Rassart, E., and Marcel, Y. L. (1997) *Biochemistry* **36,** 1798–1806
39. Brouillette, C. G., and Anantharamaiah, G. M. (1995) *Biochim. Biophys. Acta* **1256,** 103–129
40. Segrest, J. P., Jones, M. K., De Loof, H., Brouillette, C. G., Venkatachalapathi, Y. V., and Anantharamaiah, G. M. (1992) *J. Lipid Res.* **33,** 141–166
41. Smith, J. D., Waelde, C., Horwitz, A., and Zheng, P. (2002) *J. Biol. Chem.* **277,** 17797–17803
42. Gillotte, K. L., Davidson, W. S., Lund-Katz, S., Rothblat, G. H., and Phillips, M. C. (1998) *J. Lipid Res.* **39,** 1918–1928
43. Lin, G., and Oram, J. F. (2000) *Atherosclerosis* **149,** 359–370
44. Burgess, J. W., Kiss, R. S., Zheng, H., Zachariah, S., and Marcel, Y. L. (2002) *J. Biol. Chem.* **277,** 31318–31326